

THE DISCOVERY OF 1000 km s⁻¹ OUTFLOWS IN MASSIVE POST-STARBURST GALAXIES AT Z=0.6¹

CHRISTY A. TREMONTI^{2,3}, JOHN MOUSTAKAS⁴, ALEKSANDAR M. DIAMOND-STANIC²,

Draft version October 24, 2018

ABSTRACT

Numerical simulations suggest that active galactic nuclei (AGNs) play an important role in the formation of early-type galaxies by expelling gas and dust in powerful galactic winds and quenching star formation. However, the existence of AGN feedback capable of halting galaxy-wide star formation has yet to be observationally confirmed. To investigate this question, we have obtained spectra of 14 post-starburst galaxies at $z \sim 0.6$ to search for evidence of galactic winds. In 10/14 galaxies we detect Mg II $\lambda\lambda 2796, 2803$ absorption lines which are blueshifted by 490 – 2020 km s⁻¹ with respect to the stars. The median blueshift is 1140 km s⁻¹. We hypothesize that the outflowing gas represents a fossil galactic wind launched near the peak of the galaxy’s activity, a few 100 Myr ago. The velocities we measure are intermediate between those of luminous starbursts and broad absorption line quasars, which suggests that feedback from an AGN may have played a role in expelling cool gas and shutting down star formation.

Subject headings: galaxies: evolution — galaxies: ISM — galaxies: starburst — quasars: absorption lines

1. INTRODUCTION

There is mounting evidence linking quasar activity to merger-induced star formation, but the precise timing and the physical relationship between the two are not well understood (Canalizo et al. 2006). Numerical simulations suggest that mergers of gas-rich galaxies induce radial gas inflows which fuel central star formation and black hole accretion. Subsequently, feedback from the active galactic nucleus (AGN) removes the gas and dust and quenches star formation and black hole activity (e.g., Di Matteo et al. 2005). Such models have enjoyed great popularity due to their success in reproducing the present-day properties of early-type galaxies, notably the color–magnitude relation and the correlation between black hole mass and bulge stellar velocity dispersion (e.g., Granato et al. 2004; Springel et al. 2005; Menci et al. 2006). However, the existence of AGN feedback capable of halting galaxy-wide star formation has yet to be observationally confirmed.

AGN feedback is predicted to quench star formation by re-heating the cold gas and expelling much of it in powerful galactic winds. Galactic winds with velocities of 50 – 500 km s⁻¹ are commonly detected in starburst galaxies via the presence of gas absorption lines that are blueshifted relative to stellar features (e.g., Heckman et al. 2000). AGN-driven winds are expected to produce similar observational signatures, but higher outflow velocities (Thacker et al. 2006). The maximum feedback impulse is predicted to occur during the bright quasar phase. However, at this stage the quasar outshines the host galaxy, and provides a more ambiguous probe of the galaxy’s interstellar medium (ISM). (A parsec-scale cloud near the quasar would be indistinguishable from a kiloparsec-scale galactic wind.) We have therefore elected to look for remnants of AGN-driven galactic winds during the post-starburst phase, a few 100 Myr after the peak of the star

formation and AGN activity.

Post-starburst galaxies are characterized by strong stellar Balmer absorption from A-stars, but little nebular emission indicative of on-going star formation. Local post-starbursts (sometimes called ‘E+A’ or ‘K+A’ galaxies) have the kinematic and morphological signatures of pressure-supported spheroids, but frequently exhibit low surface brightness tidal tails indicative of a recent major merger (Zabludoff et al. 1996; Norton et al. 2001; Yang et al. 2004) and signs of weak AGN activity (Yan et al. 2006; Yang et al. 2006). Post-starbursts are therefore presumed to be late-stage mergers that have passed through their quasar phase and are in transition to becoming early-type galaxies. As such they provide ideal testing grounds for AGN-feedback models.

We have obtained spectra of 14 post-starbursts at $z \sim 0.6$ in order to search for evidence of galactic winds that may have played a role in shutting down star formation. We have selected galaxies at intermediate redshift because this may be an important epoch for the formation of early-type galaxies (e.g., Faber et al. 2005), and because the rest-frame near-UV is accessible in the optical. Coverage of the near-UV improves our ability to estimate the recent star formation history of our galaxies and it enables us to measure Mg II $\lambda\lambda 2796, 2803$ which is a sensitive probe of the ISM. We describe our observations in §2, the stellar populations of our post-starbursts in §3, and the outflow kinematics in §4. We discuss evidence that the wind is powered by an AGN in §5 and conclude in §6.

2. OBSERVATIONS AND DATA REDUCTION

Our sample was selected from the Sloan Digital Sky Survey (SDSS) Data Release 4 (Adelman-McCarthy et al. 2006). The parent sample is composed of $i < 20.5$ mag objects that were targeted for SDSS spectroscopy as quasar candidates, but which were subsequently classified as galaxies at $z = 0.5 – 1$. The typical signal-to-noise (S/N) ratio of the SDSS spectra is rather poor ($S/N \sim 2 \text{ pixel}^{-1}$), but sufficient for us to select a sample of galaxies for follow-up. We selected 159 objects with post-starburst characteristics — strong stellar Balmer absorption and weak nebular emission (Tremonti et al., in prep.).

We obtained higher S/N spectra of 14 galaxies with the Blue Channel Spectrograph on the 6.5-m MMT. We used

¹ Observations reported here were obtained at the MMT Observatory, a joint facility of the University of Arizona and the Smithsonian Institution.

² Steward Observatory, 933 N. Cherry Ave., Tucson, AZ 85721; tremonti@as.arizona.edu, adiamond@as.arizona.edu

³ Hubble Fellow

⁴ Center for Cosmology and Particle Physics, New York University, New York, NY 10003; jmoustakas@cosmo.nyu.edu

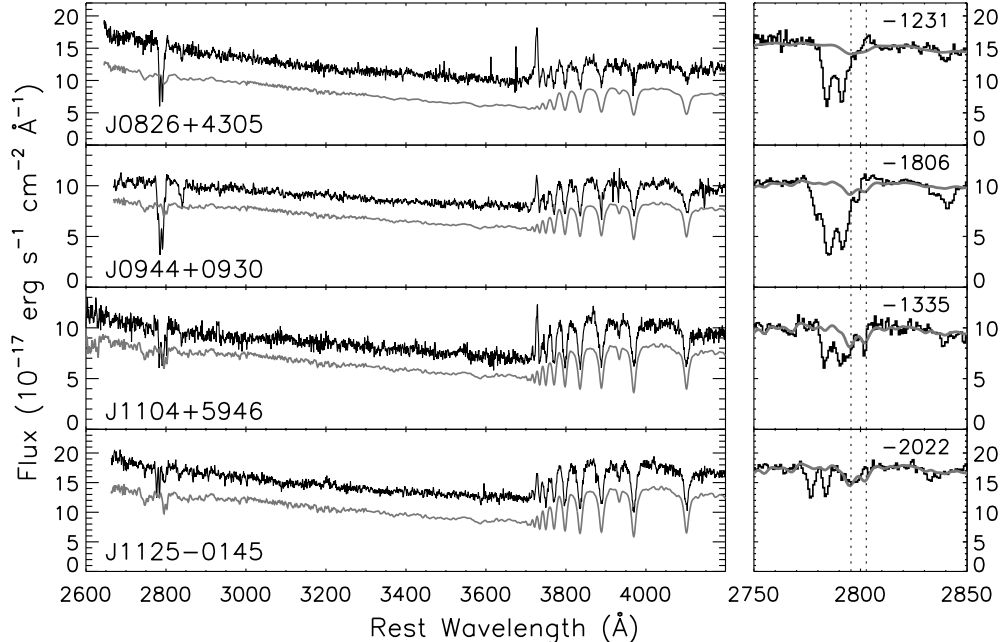


FIG. 1.— Example spectra (black) and continuum model fits (gray). In the lefthand panel, the continuum models are offset for clarity. The righthand panel highlights the region around the Mg II doublet. Dotted lines mark the rest wavelength of Mg II. The presence of blueshifted lines indicates an outflow. The velocity of the most blueshifted component is given in km s^{-1} in the upper right corner.

the 500 line mm^{-1} grating blazed at 5600 \AA which gave us spectral coverage from $4050 - 7200 \text{ \AA}$ with a dispersion of 1.19 \AA per pixel. For our $z = 0.51 - 0.75$ galaxies, this yielded rest-frame coverage from $2700 - 4100 \text{ \AA}$. Because most of our objects are unresolved in the SDSS imaging we used a $1''$ slit, which yielded a FWHM resolution of $\sim 3.6 \text{ \AA}$. The spectra were reduced, extracted, and spectrophotometrically calibrated using the ISPEC2D data reduction package (Moustakas & Kennicutt 2006). The MMT spectra show good agreement with the SDSS data, but have $S/N = 15\text{--}30 \text{ pixel}^{-1}$. Spectra of four representative galaxies are shown in Figure 1.

3. STELLAR POPULATION

We detect significant Mg II $\lambda\lambda 2796, 2803$ absorption in all of our galaxies. Mg II is one of the strongest interstellar resonance absorption lines; however, it is also present in the atmospheres of A-stars and later spectral types. Hence to accurately measure the ISM absorption lines, we must carefully model the stellar continuum. We use the Bruzual & Charlot (2003, hereafter BC03) stellar population synthesis models to create synthetic spectra for different star formation histories. We assume super-solar metallicity ($Z=2.5 Z_{\odot}$) since Oxygen abundances several times solar are measured in comparably luminous star forming galaxies at $z \sim 0.6$ (Lamareille et al. 2006). We adopt a star formation history designed to emulate a major merger between gas-rich disk galaxies. Following the starburst, star formation decays exponentially with time constants ranging from $\tau_{burst}=25 - 500 \text{ Myr}$. We fit each of our spectra with a grid of models spanning a range of ages, τ_{burst} , and reddening values and adopt the model with the minimum χ^2 as the best fit. In several cases to achieve an optimal fit it was necessary to add an additional power-law component which may represent a featureless quasar continuum (see §5).

A byproduct of our stellar continuum modeling is an estimate of the stellar mass, the time since the peak star formation event (t_{burst}), and how quickly star formation ceased (τ_{burst}). These parameters and their uncertainties will be discussed fully in Tremonti et al., in prep. Our modeling suggests that the galaxies are massive ($0.7 - 4.8 \times 10^{11} M_{\odot}$) and have recently experienced a burst ($t_{burst} = 75 - 300 \text{ Myr}$) that faded rapidly ($\tau_{burst} = 25 - 100 \text{ Myr}$). The short starburst timescales imply strong feedback from supernovae or an AGN.

4. GAS KINEMATICS

We use our best-fit synthetic spectra to correct for the contribution of stellar absorption to the Mg II lines. At wavelengths less than 3300 \AA , the BC03 models use the Pickles (1998) stellar library which has a spectral resolution of 10 \AA . This resolution is too low to adequately model the Mg II doublet in our data. We circumvent this problem by patching the BC03 models in the $2600 - 3300 \text{ \AA}$ range using theoretical stellar spectra from the UVBLUE stellar library (Rodríguez-Merino et al. 2005). The rightmost panel in Figure 1 shows our continuum fits in the $2750 - 2850 \text{ \AA}$ region. In many cases the ISM lines are so strong or blueshifted that the stellar component of Mg II is unimportant. However, in a few galaxies stellar Mg II is dominant. After correcting for the stellar light we find that 10 of our 14 galaxies have measurable Mg II absorption. The equivalent widths (EWs) of interstellar Mg II range from $0.8 - 10.4 \text{ \AA}$ (see Table 1).

After correcting for the stellar contribution to Mg II, we fit the ISM absorption lines following Rupke et al. (2005a). In the optically thin case the doublet ratio is 2:1, but in our data the lines are moderately saturated. At our spectral resolution ($\sim 100 \text{ km s}^{-1}$) this produces degeneracies between the optical depth at line center, the covering factor, and the Doppler b parameter. However, velocities can be measured

robustly. The lines have a median Doppler width of $b = 260 \text{ km s}^{-1}$, although it is possible that they include narrower unresolved components. In six of the galaxies we fit two absorption components. Three galaxies display a P-Cygni profile — blueshifted absorption coupled with redshifted emission which may originate on the back side of an expanding shell. We model the emission with a Gaussian. In Table 1 we list the measured absorption-line velocities. We denote the velocity of the most blueshifted component in each spectrum as v_{max} . We compute the average velocity, v_{avg} , weighting the components by their EWs. The median values for the sample are $v_{avg} = -920 \text{ km s}^{-1}$ and $v_{max} = -1140 \text{ km s}^{-1}$.

We hypothesize that the blueshifted Mg II lines originate in galactic winds that were launched near the peak of the galaxies’ starburst activity a few 100 Myr ago. An alternate interpretation is that the absorbing gas is tidal debris associated with the merger. However, the inner parts of tidal tails are expected to be bound and to fall back within a few 100 Myr (Hibbard & Mihos 1995), whereas we detect outflows. In addition, gaseous tidal tails are confined to relatively thin streams with small global covering factors; therefore it seems unlikely that we would detect tidal gas in absorption in 70% of our sources. Hence we conclude that the blueshifted Mg II lines originate in fossil galactic winds.

5. DISCUSSION

Our $z \sim 0.6$ post-starburst galaxies rank among the most luminous and massive galaxies in the universe ($M_B = -22.5$ – -23.7 mag , $M_* = 0.7$ – $4.8 \times 10^{11} M_\odot$; Table 1) and they offer a rare window on the formation of today’s massive early-type galaxies. The detection of interstellar Mg II in 10 of our 14 galaxies enables us to probe the properties of the cold ISM. We find evidence for strong outflows in all 10 systems, with velocities in the range $v_{max} = 500$ – 2000 km s^{-1} . The median v_{max} of the sample is 1140 km s^{-1} , which exceeds the 400 – 600 km s^{-1} velocities typical of luminous starburst galaxies (Heckman et al. 2000). We put these outflows in context in Figure 2 where we plot absolute B -band magnitude versus ISM outflow velocity for a variety of systems. We include local starbursts (Schwartz & Martin 2004; Schwartz et al. 2006), Luminous and Ultra-Luminous Infrared Galaxies (LIRGs/ULIRGs; Rupke et al. 2005b), and $z \sim 3$ Lyman Break Galaxies (LBGs; Pettini et al. 2001). We augment this sample with starburst/AGN composite ULIRGs from Rupke et al. (2005c) and a sample of Low-ionization Broad Absorption Line quasars (LoBALs) from the SDSS (Trump et al. 2006). LoBALs are characterized by broad Mg II absorption troughs. They are more common in infrared-selected than optically-selected quasar samples (Boroson & Meyers 1992), which has led to the suggestion that LoBALs are quasars in the process of removing their natal cocoons of gas and dust.

Figure 2 shows a striking trend for more luminous galaxies to have higher outflow velocities. Similar trends have been noted previously. In starbursts, Rupke et al. (2005b) and Martin (2005) found strong correlations between outflow velocity and galaxy mass and star formation rate. Our post-starburst galaxies have extraordinarily high outflow velocities when compared to their natural analogs, starburst-powered ULIRGs and LBGs. Their outflow velocities are comparable to some of the AGN composite ULIRGs, and at the lower end of the range observed for LoBAL quasars. This result implies that our post-starburst galaxies may harbor both fading

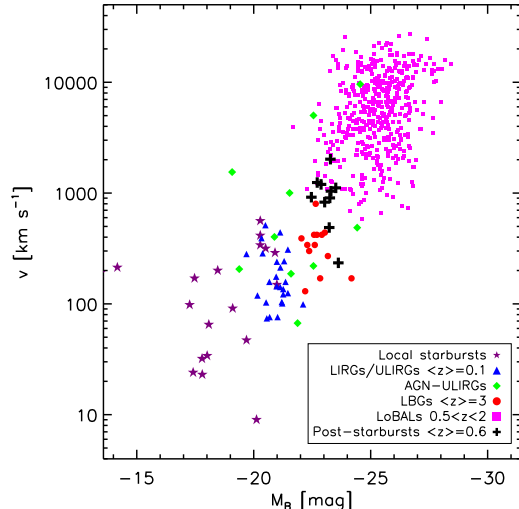


FIG. 2.— Outflow velocity versus absolute B -band magnitude. Our post-starburst galaxies (black plus signs) have velocities intermediate between luminous starbursts and LoBAL quasars. References for the various samples are given in the text.

starbursts and fading quasars. Evidence for the presence of an AGN can also be found in the spectra. In massive metal-rich galaxies the narrow emission line [O III] $\lambda 5007$ is relatively uncontaminated by star formation and a good tracer of the AGN’s bolometric luminosity (Heckman et al. 2005). We are able to detect [O III] lines in four of our galaxies using the SDSS spectra. The galaxies have $EW_{[OIII]} = 6$ – 9 \AA and $L_{[OIII]} = 0.4$ – $4 \times 10^8 L_\odot$, placing them in the regime of powerful AGN. One of the four also shows [Ne V] $\lambda 3426$ emission, which is an unequivocal signpost of AGN activity.

We achieve better continuum fits to six of our galaxies (three of which have [O III] emission) when we add a featureless power-law component ($F_\lambda \propto \lambda^{\alpha_\lambda}$) with a spectral slope of $\alpha_\lambda = -1.6$, which is typical of quasars (Vanden Berk et al. 2001). Without the power-law, high present-day star formation rates are implied, which is at odds with the lack of strong Balmer emission. The very blue UV continua of these galaxies rules out high dust attenuation as a means of quenching the nebular lines. In our best-fit models the power-law supplies 40–70% of the flux at 3000 \AA . Curiously, despite the moderate dilution of the AGN continuum by the galaxy, few spectral features characteristic of Type 1 quasars are detected. We are able to rule out strong broad $H\beta$ emission lines on the basis of the SDSS spectra. Broad Mg II (FWHM $\sim 8000 \text{ km s}^{-1}$) is present at a low level in SDSS J214000.49+120914.6, but absent in the other spectra. The physical reason for the lack of broad lines in our AGN-post-starburst composites is unclear.

Mechanical energy from AGN radio jets has been suggested as a power source for large-scale outflows (e.g., Nesvadba et al. 2006). For 13/14 galaxies, radio data are available from the Faint Images of the Radio Sky at Twenty cm survey (FIRST; Becker et al. 1995). Two galaxies are detected ($F_{1.4\text{GHz}} = 12, 20 \text{ mJy}$) down to a limit of $\sim 1 \text{ mJy}$. These two sources show no optical signs of AGN activity, but have sufficient radio power to be classed as radio-loud AGN (Kellermann et al. 1989). Neither galaxy hosts an outflow, thus, preliminary evidence disfavors radio jets as the driving mechanism.

It is interesting to consider whether the outflows we observe

could have been the direct cause of the abrupt drop in the star formation rate of our galaxies a few 100 Myr ago. This seems plausible if the winds entrained a large fraction of the cold ISM. We can crudely estimate the mass in the outflow using the Mg II column density that we derive. Because the error bars on some individual measurements are large, we use the median value, $N(\text{Mg}^+) = 8.1 \times 10^{14} \text{ cm}^{-2}$, in our calculations. The presence of a weak Mg I $\lambda 2852$ line in some of the spectra implies an ionization correction of $\sim 3\%$. We translate our Mg column into a total gas column by accounting for depletion onto dust grains ($X = -1.4$; Savage & Sembach 1996) and assuming a Mg/H ratio 2.5 times the solar value. In this way we infer $N(\text{H}) = 2 \times 10^{20} \text{ cm}^{-2}$, which is consistent with the median value found for high- z ULIRGs (Rupke et al. 2005b).

The total mass in the outflow depends strongly on how far away the absorbing gas is from the galaxy. Following Rupke et al. (2005b), we assume that the wind is a shell-like structure that covers 80% of the optically luminous galaxy. To calculate the outer radius of the shell, r_{out} , we adopt a simple picture where the wind is launched at the peak of the star formation and AGN activity and moves at constant velocity. Using the median values of the burst age ($t \simeq 100$ Myr) and outflow velocity ($v \simeq 1000 \text{ km s}^{-1}$), we find $r_{out} = vt = 100$ kpc. The shell's thickness depends on the duration of the outflow. We consider two limiting cases: a thick shell with an inner radius $r_{in} = 1$ kpc, and a thin shell with $r_{in} = 99$ kpc. Rupke's equation (4) yields masses of $M_{wind} = 10^9$ and $10^{11} M_{\odot}$ for the thick and thin cases respectively, implying that between 1 and 50% of the galaxies' baryons are in the outflow. The wind mass estimated for the thin shell is probably too large: simulations of starburst and AGN feedback require highly efficient and energetic winds to unbind more than 25% of the galaxy's initial gas mass (Cox et al., in prep).

Another possibility we must consider is that the Mg II absorber is local to the AGN and does not extend to kiloparsec scales. In this case the wind is unlikely to have played a significant role in regulating star formation. For six of our galaxies this possibility cannot be ruled out because our estimate of the Mg II covering factor is less than or equal to the amount of continuum light contributed by the AGN. We obtained data with $5\times$ higher spectral resolution for SDSS J082638.41+430529.5 in order to obtain a better measurement

of the covering factor. In the high resolution spectrum, the Mg II absorption is near-black at line center, implying that the absorber covers both the AGN and the stars. We also detect strong Mg II absorption in three galaxies with no contribution to the continuum from an AGN. Hence, in 4/10 galaxies we can confirm that the winds are galaxy-scale features indicative of energetically significant feedback events. Constraints on the remaining galaxies await higher resolution spectra.

6. CONCLUSIONS

To test currently popular models of early-type galaxy evolution that incorporate feedback from AGN, we have looked for the presence of galactic winds in a sample of massive post-starburst galaxies at $z = 0.5 - 0.75$. We detect interstellar Mg II which is blueshifted by 500 - 2000 km s^{-1} in 10/14 galaxies. These outflow velocities are intermediate between those of luminous starbursts and LoBAL quasars, which suggests that feedback from an AGN may have played a role in powering the outflow. In 4/10 galaxies we can confirm that the outflows are energetically significant galaxy-wide events, and not phenomena local to the AGN. We estimate that the outflows reach distances of ~ 100 kpc and contain upwards of $10^9 M_{\odot}$ of gas. We conclude that AGN are likely to have played a major role in causing the abrupt truncation of star formation in these massive galaxies.

We thank Tim Heckman for helpful discussions and Kevin Luhman for contributing telescope time. We are grateful to the Aspen Center for Physics for hospitality while part of this work was completed. Support for C. A. T. was provided by NASA through Hubble Fellowship grants HST-HF-01192.01 awarded by the Space Telescope Science Institute, which is operated by the Association of Universities for Research in Astronomy, Inc., for NASA, under contract NAS5-26555.

Funding for the Sloan Digital Sky Survey (SDSS) has been provided by the Alfred P. Sloan Foundation, the Participating Institutions, the National Aeronautics and Space Administration, the National Science Foundation, the U.S. Department of Energy, the Japanese Monbukagakusho, and the Max Planck Society. The SDSS Web site is <http://www.sdss.org/>.

REFERENCES

- Adelman-McCarthy, J. K., et al. 2006, *ApJS*, 162, 38
 Becker, R. H., White, R. L., & Helfand, D. J. 1995, *ApJ*, 450, 559
 Boroson, T. A., & Meyers, K. A. 1992, *ApJ*, 397, 442
 Bruzual, G., & Charlot, S. 2003, *MNRAS*, 344, 1000
 Canalizo, G., Stockton, A., Brotherton, M. S., & Lacy, M. 2006, *New Astronomy Review*, 50, 650
 Di Matteo, T., Springel, V., & Hernquist, L. 2005, *Nature*, 433, 604
 Faber, S. M., et al. 2005, *ArXiv Astrophysics e-prints*, arXiv:astro-ph/0506044
 Granato, G. L., De Zotti, G., Silva, L., Bressan, A., & Danese, L. 2004, *ApJ*, 600, 580
 Heckman, T. M., Lehnert, M. D., Strickland, D. K., & Armus, L. 2000, *ApJS*, 129, 493
 Heckman, T. M., Ptak, A., Hornschemeier, A., & Kauffmann, G. 2005, *ApJ*, 634, 161
 Hibbard, J. E. & Mihos, J. C. 1995, *AJ*, 110, 140
 Kellermann, K. I., Sramek, R., Schmidt, M., Shaffer, D. B., & Green, R. 1989, *AJ*, 98, 1195
 Lamareille, F., Contini, T., Brinchmann, J., Le Borgne, J.-F., Charlot, S., & Richard, J. 2006, *A&A*, 448, 907
 Martin, C. L. 2005, *ApJ*, 621, 227
 Menci, N., Fontana, A., Giallongo, E., Grazian, A., & Salimbeni, S. 2006, *ApJ*, 647, 753
 Moustakas, J., & Kennicutt, R. C., Jr. 2006, *ApJS*, 164, 81
 Nesvadba, N. P. H., Lehnert, M. D., Eisenhauer, F., Gilbert, A., Tecza, M., & Abuter, R. 2006, *ApJ*, 650, 693
 Norton, S. A., Gebhardt, K., Zabludoff, A. I., & Zaritsky, D. 2001, *ApJ*, 557, 150
 Pettini, M., Shapley, A. E., Steidel, C. C., Cuby, J.-G., Dickinson, M., Moorwood, A. F. M., Adelberger, K. L., & Giallisco, M. 2001, *ApJ*, 554, 981
 Pickles, A. J. 1998, *PASP*, 110, 863
 Rodríguez-Merino, L. H., Chavez, M., Bertone, E., & Buzzoni, A. 2005, *ApJ*, 626, 411
 Rupke, D. S., Veilleux, S., & Sanders, D. B. 2005, *ApJS*, 160, 87
 Rupke, D. S., Veilleux, S., & Sanders, D. B. 2005, *ApJS*, 160, 115
 Rupke, D. S., Veilleux, S., & Sanders, D. B. 2005, *ApJ*, 632, 751
 Savage, B. D., & Sembach, K. R. 1996, *ARA&A*, 34, 279
 Schwartz, C. M., & Martin, C. L. 2004, *ApJ*, 610, 201
 Schwartz, C. M., Martin, C. L., Chandar, R., Leitherer, C., Heckman, T. M., & Oey, M. S. 2006, *ApJ*, 646, 858
 Springel, V., Di Matteo, T., & Hernquist, L. 2005, *ApJ*, 620, L79
 Thacker, R. J., Scannapieco, E., & Couchman, H. M. P. 2006, *ApJ*, 653, 86
 Trump, J. R., et al. 2006, *ApJS*, 165, 1
 Vanden Berk, D. E., et al. 2001, *AJ*, 122, 549

TABLE 1

SDSS Galaxy Name	z	M_B (mag)	$\log M_*$ (M_\odot)	Mg II EW (\AA)	v_{avg} (km s^{-1})	v_{max} (km s^{-1})
J081150.09+471615.2	0.515	-22.5	11.0	2.5	-918 ± 27	-918 ± 27
J082638.41+430529.5	0.603	-23.3	10.9	4.8	-1040 ± 42	-1232 ± 09
J082733.88+295451.3	0.681	-23.1	11.3
J094417.85+093019.4	0.514	-22.7	10.8	7.9	-1245 ± 10	-1807 ± 13
J103906.97+453754.1	0.634	-23.3	11.1	4.1	-904 ± 31	-1342 ± 40
J110437.46+594639.6	0.573	-22.9	10.9	3.4	-1197 ± 35	-1335 ± 22
J112518.90-014532.5	0.519	-23.3	11.1	1.9	-2022 ± 10	-2022 ± 10
J114257.23+603711.2	0.568	-23.6	11.5
J124807.16+060111.8	0.632	-23.2	11.2	2.9	-489 ± 18	-489 ± 18
J150636.30+540220.9	0.608	-23.5	10.9	2.5	-1114 ± 66	-1135 ± 78
J160413.25+393931.4	0.564	-23.6	11.7
J163541.72+470924.5	0.699	-23.7	11.5
J171300.39+281708.2	0.577	-23.0	11.2	0.8	-828 ± 35	-828 ± 35
J214000.49+120914.6	0.751	-23.6	11.2	10.4	-234 ± 40	-573 ± 48

NOTE. — We assume $\Omega_M = 0.3$, $\Omega_\Lambda = 0.7$, and $H_0 = 70 \text{ km s}^{-1} \text{ Mpc}^{-1}$. M_B is k -corrected to $z = 0$ and on the Vega system. The Mg II EWs are for the interstellar component and are measured in the rest frame. The velocities v_{max} and v_{avg} are defined in §4.

Yan, R., Newman, J. A., Faber, S. M., Konidaris, N., Koo, D., & Davis, M. 2006, *ApJ*, 648, 281
 Yang, Y., Zabludoff, A. I., Zaritsky, D., Lauer, T. R., & Mihos, J. C. 2004, *ApJ*, 607, 258
 Yang, Y., Tremonti, C. A., Zabludoff, A. I., & Zaritsky, D. 2006, *ApJ*, 646, L33

Zabludoff, A. I., Zaritsky, D., Lin, H., Tucker, D., Hashimoto, Y., Shectman, S. A., Oemler, A., & Kirshner, R. P. 1996, *ApJ*, 466, 104